UCRL-JC-124876
PREPRINT

Laser Induced Damage and Fracture in Fused Silica Vacuum Windows

J. H. Campbell, P. A. Hurst, D. D. Heggins, W. A. Steele, and S. E. Bumpas

This paper was prepared for submittal to the 28th Annual Symposium on Optical Materials for High Power Lasers '96 Boulder, CO October 7-9, 1996

November 20, 1996

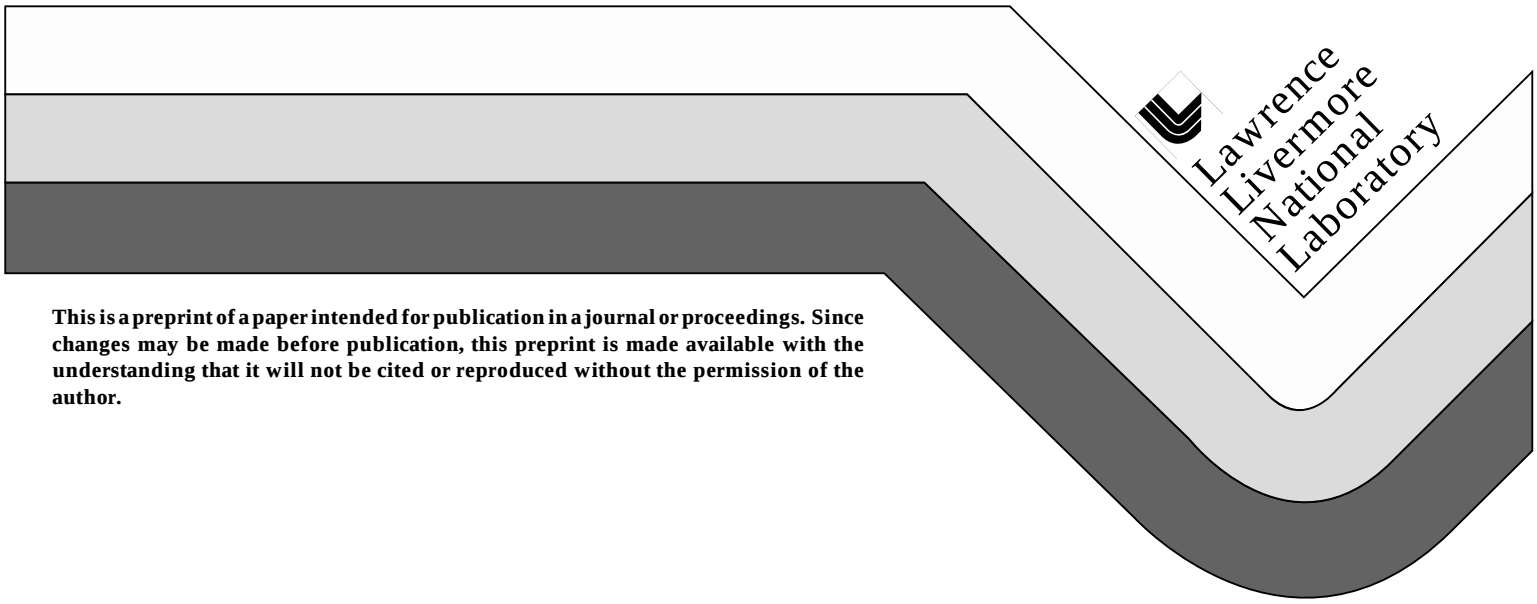

Laser induced damage and fracture in fused silica vacuum windows

John H. Campbell, Patricia A. Hurst, Dwight D. Heggins,
William A. Steele and Stanley E. Bumpas

Lawrence Livermore National Laboratory
P.O. Box 808
Livermore, California 94551

ABSTRACT

Laser induced damage, that initiates catastrophic fracture, has been observed in large (up to 61-cm diameter), fused silica lenses that also serve as vacuum barriers in high-fluence positions on the Nova and Beamlet lasers. In nearly all cases damage occurs on the vacuum (tensile) side of the lens. The damage can lead to catastrophic crack growth if the flaw (damage) size exceeds the critical flaw size for SiO_2. If the elastic stored energy in the lens is high enough, the lens will fracture into many pieces resulting in an implosion. The consequences of such an implosion can be severe, particularly for large vacuum systems. Three parameters control the degree of fracture in the vacuum barrier window: 1) the elastic stored energy (i.e. tensile stress) 2) the ratio of the window thickness to flaw depth and 3) secondary crack propagation. Fracture experiments have been carried out on 15-cm diameter fused silica windows that contain surface flaws caused by laser damage. The results of these experiments, combined with data from window failures on Beamlet and Nova have been used to develop design criteria for a “fail-safe” lens (that is, a lens that may catastrophically fracture but will not implode). Specifically the window must be made thick enough such that the peak tensile stress is less than 500 psi (3.4 MPa) and the corresponding ratio of the thickness to critical flaw size is less that 6. Under these conditions a properly mounted window, upon failure, will break into only two pieces and will not implode. One caveat to these design criteria is that the air leak through the window fracture and into the vacuum must be rapid enough too reduce the load on the window before secondary crack growth occurs. Finite element stress calculations of a window before and immediately following fracture into two pieces show that the elastic stored energy is redistributed if the fragments “lock” in place and thereby bridge the opening. In such cases, the peak stresses at the flaw site can increase leading to further (i.e. secondary) crack growth.

Key words: fused silica, laser damage, glass fracture, spatial filter lens

1. INTRODUCTION

The large laser systems used for inertial confinement fusion research contain a number of vacuum vessels along the propagation path of the high energy beam.[1-3] Most of the vacuum vessels are spatial filters that serve to image relay the beam through the system and remove high spatial frequency noise. In addition a large vacuum chamber at the end of the propagation path contains the laser target that is irradiated by the beam(s). Fused silica lenses and windows serve the dual function of optical element and vacuum barrier on these chambers. For example, Fig. 1 shows a me-

chanical engineering drawing of the end of the Beamlet spatial filter housing and the 61-cm diameter fused silica lens that also serves as a vacuum barrier. The lens is mounted on a pliable rubber seal (o-ring) that keep the lens from contacting the precision metal surface of the mounting flange. A retaining ring gently holds the lens in place until the vacuum load is applied pulling the lens down onto the rubber o-ring. With this mounting design the only stress applied to the lens is from the vacuum load.

The volume of the spatial filter vacuum chambers on currently operating lasers at LLNL (Nova and Beamlet) range from a few liters to as high as about 5 m^3 for the 18 m long spatial filter housing used on the Beamlet laser. The Nova final target chamber also has a volume of nearly 5 m^3. The volume of the vacuum system is important because it determines the P•V energy released (i.e. potential destructive force) in the event of a catastrophic failure of a vacuum barrier window or lens; this energy is about 10^5 J/m^3.

Future laser systems, such as the 1.8 MJ NIF laser, planned to be operational in 2002,[2] will use very large vacuum spatial filters and a vacuum target chamber. The 10-m diameter NIF target chamber has a volume of about 500 m^3 corresponding to about 50 MJ of potential energy. Thus, a catastrophic implosion of a vacuum barrier window would have enormous destructive impact on the equipment inside or in the immediate vicinity the target chamber. In addition the rush of air to fill the vacuum chamber could have serious effects on mechanical and optical structures further removed from the chamber. The potential personnel hazard is, of course, obvious.

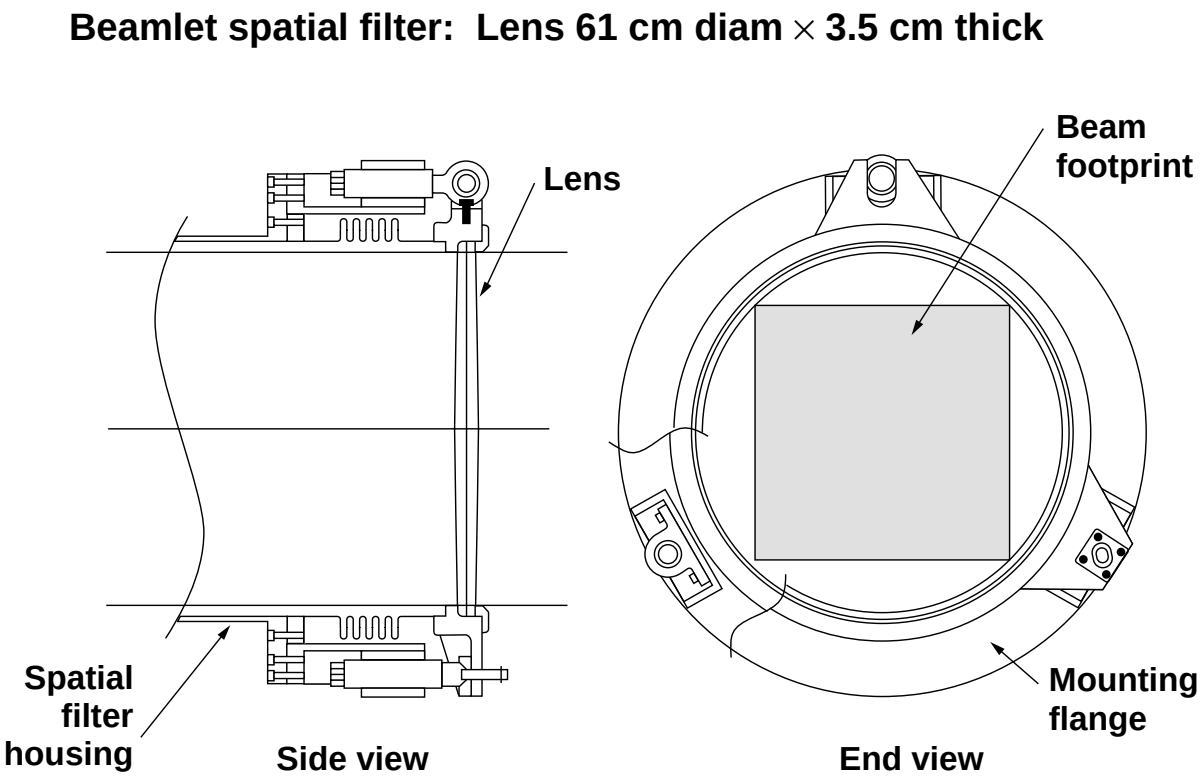

Figure 1. Schematic view of the Beamlet spatial filter housing showing the 61-cm diameter x 3.5-cm thick fused silica lens that also serves as a vacuum barrier.

The hazards of large vacuum systems are well know and it is possible to mechanically design safe systems. In general the lenses and windows are designed to be sufficiently thick that the tensile stress on the vacuum side remains far below the tensile strength of the polished fused silica substrate. However, one must also account for the potential of laser induced optical damage to the tensile surface of the window that can significantly reduce the strength of the glass. In practice the lens or window is usually made somewhat thicker in order to account for laser damage. Currently there are no firm design rules governing how thick the lens should be made, instead the thickness is chosen largely based on experience and anecdotal evidence gained through past laser operations.

Unfortunately, making the lens thicker adversely affects the beam quality at high intensities. This is due to the non-linear phase retardance that occurs in the material at high intensity.[4,5,6] The magnitude of the phase retardance is characterized by the "B integral" given by the expression:

$$B = \frac{2\pi}{\lambda}\int_0^L \gamma\, I\, dx \qquad (1)$$

where B is the cumulative phase retardance (in radians) which is proportional to the non-linear index coefficients (γ) (cm^2/GW) of the optical materials in the propagation path of length L. Note that B depends inversely on the operating wavelength of the laser, λ, therefore non-linear effects on the beam quality become particularly troublesome after frequency conversion. This is due to both the shorter wavelength and the fact that frequency conversion occurs at the output of the laser where the intensity, I (GW/cm^2), is highest. The B integral is taken over the optical path length between spatial filters and therefore the intensity may vary along the path due to the optical gain or loss from various components.

Intensity noise and/or ripple on the propagating beam grows as exp (2B). This noise growth eventually causes the beam to break-up into small, high intensity regions with a characteristic spatial frequency. This break-up is often visible as an "orange-peel" like structure in the near field image of the beam. The design criteria for ICF high peak-power lasers is that $B \leq 2$ radians.[7] It is clear that in the high intensity stages of the laser it is highly desirable to make the optical materials as thin as possible. This is particularly true for the lenses of the final spatial filter and the target chamber.

During the course of high fluence laser operation we have observed laser induced damage on the vacuum surface of certain lenses of both Nova and Beamlet.[8] In particular the input lenses of the final spatial filters see the highest 1ω fluence and experience the most damage. The laser induced damage often grows on subsequent laser shots until it exceeds the critical flaw size for the material causing the lens to catastrophically fail. In the case of Nova, the 52-cm diameter by 3.7 cm thick lenses fracture into 2 or 3 pieces that lock in place by "bridging" across the opening of the spatial filter. In this failure mode the vacuum then slowly comes up to ambient pressure by air leaking through the fractures. No mechanical damage is experienced during these failures and over more than 10 years of operation on Nova approximately 20 lenses have fractured in this fashion. In stark contrast however, is our experience on Beamlet; on two occasions we observed laser induced fracture and failure of the 61-cm diameter by 3.5-cm thick spatial filter lens in which the fracture pieces did not lock in place but imploded causing severe damage to the mechanical and optical assemblies in the spatial filter.

In a previous paper [8] we discussed the lens failures observed on Beamlet and Nova and the possible sources for laser damage that lead to failure. In this paper we discuss the results of experiments carried out on 15 cm fused silica test plates. Our goal is to develop a set of vacuum window/lens design rules based on sound material science principles. These results are used to further analyze the lens failures on Nova and Beamlet and to develop a "fail-safe" lens design for use on NIF.

2. SOME GENERAL PRINCIPLES GOVERNING FRACTURE IN GLASS PLATES

The strength and fracture of glass has been the subject of considerable study because of it's great practical importance (see for example references 9,10 and citations contained therein). Well known fracture mechanics principles can be used to describe both the generation and growth of fractures in a glass body. In addition the markings on the surfaces of failed glass parts can be analyzed to determine the source and size of the initiating flaw, the direction of crack propagation, relative velocities of different fractures, the initial state of stress, etc.[11,12]

The size of a flaw at the surface of a glass body (or any brittle material) can be related to stress at failure using the Griffith fracture criteria:

$$a = f_s \left(\frac{K_{1c}}{\sigma_t} \right)^2 \qquad (2)$$

where a is the characteristic size of the surface flaw, K_{lc} the fracture toughness ($m^{l/2} \cdot Pa$) and σ_t the tensile strength (Pa) of the brittle material. The factor f_s accounts for the shape of the flaw; for the work here we use a value of $1/\pi$ that assumes a "half-penny" fracture shape. This agrees with our observation of the crack shape in cases of slow crack growth to failure. In addition this case gives a somewhat conservative estimate of the maximum flaw size at failure compared to other flaw geometries and shape factors.

During fracture of brittle materials, the energy used to produce new surfaces is proportional to the elastic stored energy, E_s, in the material. In turn, the stored energy is related to the stress via the expression:

$$E_s = \int_o^{V_L} \sigma \cdot \varepsilon \, dV$$

where σ is the stress (Pa), ε the strain (m) and V_L the integrated volume (m^3) of the elastic material under the applied stress. The strain is related to stress via a Hook's law relationship:

$$\sigma = E \, \varepsilon \qquad (4)$$

where E is the Youngs modulus (Pa) of the material. Therefore, after substituting eq. 4 into 3 and integrating it is straight forward to show that stored energy is proportional to the square of the stress:

$$E_s = k\sigma^2 V_L / E \qquad (5)$$

As stated above, the fracture area produced on failure is linearly proportional to the stored energy and thus eq. 5 can be rewritten in the more useful form:

$$A_f = k' \sigma^2 V_L / E \tag{6}$$

where k and k´ in eqs. 5 and 6 are constants.

Equation 6 provides a useful scaling relationship for estimating the fracture area for geometrically similar objects under comparable loading conditions. For example, in a previous publication[8] we estimated the fracture area produced under given stress conditions for Nova lenses and used that to estimate the area generated during fracture of a Beamlet lens. This is because the Nova and Beamlet lenses are comparably shaped and have similar vacuum loading (although the stored energy varies significantly). This empirically determined scaling relationship is given by:

$$A_f = 6.6 \times 10^{-4} \sigma_p^{\,2} (V_L / V_N) \tag{7}$$

where A_f is the generated fracture area (cm^2) on failure, σ_p the peak tensile stress (psi) in the lens and V_L/V_N is a volume normalization factor where V_N is the volume of the Nova lens and V_L the volume of the lens under test. The numerical constant in equation 7 has units of cm^2/psi^2 and was empirically determined from the fracture data for eight Nova lenses. Later in this report we show that this simple expression accurately predicts the fracture area for both small test plates (15-cm dia.) as well as the large Beamlet lens (61-cm dia.).

In designing glass vacuum windows it is important to bare in mind that for identical pressure loading the peak tensile stress varies as the square of the aspect ratio $(d/t)^2$ where d is the window diameter and t the thickness. It is obvious from eq. 2 that the critical flaw size for failure varies as $(t/d)^4$. In other words slightly increasing the thickness of a given window dramatically reduces the chance for failure. However, as explained above one desires the thinnest possible optics for high intensity laser applications. It is these opposing design principles that make the design of high power laser vacuum windows and lens so difficult.

During failure the elasticity stored energy in the glass plate is distributed into three main components: energy to create new surfaces (fracture), audio energy (noise) and heat; (heat includes the kinetic energy of the fragments):

$$E_s = E_{fract} + E_{audio} + E_{heat} \tag{8}$$

The fracture energy is given by:

$$E_{fract} = \gamma_s A_f \tag{9}$$

where γ_s is the surface energy (J/m^2) and A_f is the fracture area (m^2). Fused silica has a surface energy of about 4.3 J/m^2. A good rule-of-thumb is that the energy used to form new surfaces (frac-

tures) is generally less than 10% of the stored energy. For pieces of glass having the same approximate shape we assume that the fraction of stored energy distributed into forming new surfaces will remain nearly constant.

3. EXPERIMENTAL SYSTEM.

A schematic diagram of the experimental system used to measure fracture in the glass test plates is shown in Fig. 2. The glass plate is mounted on an o-ring seal in the vacuum vessel. The volume of the vacuum system is minimized by adding a metal spacer and a soft pad directly beneath the glass. This reduces the stored energy in the vacuum thereby minimizing this energy contribution to the generation of new fractures in the event the glass pieces implode. A vacuum gauge reads the pressure ($\pm$ 0.1 torr) and a video camera records the pressure at the time of failure. The test system can accommodate glass plates 15-cm in diameter varying in thickness from 1.6 to 9.6 mm.

Flaws are generated on the glass surface using the output from a frequency tripled (355 nm) Nd-YAG laser operating at a pulse length of 3 ns and a repetition rate of about 1 Hz. A small scratch is used to initiate the damage on the surface of the glass. After about 50 to 100 shots this surface damage grows to approximately 1 cm in diameter and 3 mm deep; the fracture pattern (i.e. crater) resembles that created by particle impact on a glass surface. Recent results from Feit et al.[13] show that the over-pressure generated by the shock wave produced during laser damage is sufficient to create such a fracture crater. Multiple laser shots cause this fracture site to grow in depth at the rate of about 30 um/shot; this agrees with predictions by Feit et al. The flaw depth is generally less than the flaw radius and is typically one-half to two-thirds the radius.

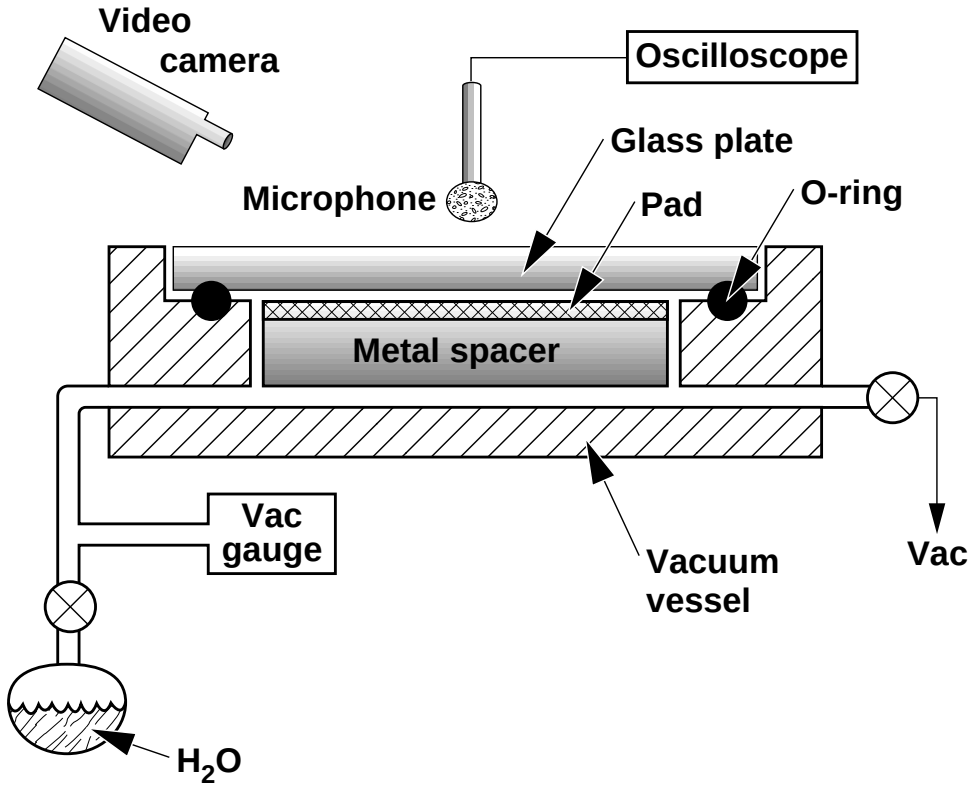

Figure 2. Schematic drawing of the experimental system used to measure catastrophic fracture in 15-cm diameter glass test plates.

For many of the test pieces the flaw that was generated during laser damage was less than the critical flaw size needed to cause catastrophic failure when subjected to full vacuum load. Therefore we included a means for adding water vapor to the chamber to promote slow crack growth to the critical flaw size (see Fig. 2). The effect of water on slow crack growth in glass is well known (see, for example, the pioneering work by Weiderhorn).[14]

A microphone was added in later tests to record the magnitude of the audio signal. The microphone was an AKG Acoustics model C 1000 S, with a nearly flat-top response over the frequency range of 50 to 20,000 Hz. The output from the microphone was used to trigger an oscilloscope. The peak voltage recorded at the start of a damped-sinusodial-like transient decay was used as a measure of the strength of the audio energy produced during fracture.

Test plates were fabricated from two different glasses: fused silica (Corning code 7940) and a multi-component borosilicate glass (Pilkington extra white strip). The surfaces of the glass plates were polished; pressure tests conducted on samples without laser induced damage show tensile strengths greater than 10,000 psi (68 MPa).

4. RESULTS AND DISCUSSION

A. Tests on 15-cm disks

The results from the fracture tests on 15-cm diameter fused silica disks are shown in Figs. 3 and 4. The data are for plates ranging in thickness from 1.6 to 6.4 mm. The data in Fig. 3 show a clear linear relationship between the total area of the fracture surfaces produced and the square of the stress as predicted by eq. 6.

By rearranging eq. 6:

$$A_f / \sigma^2 = k' V_L \qquad (10)$$

one can show that the slopes of the lines in Fig. 3 (i.e. A_f / σ^2) should vary linearly with the sample volume. A plot of this data is given in Fig. 4; although there seems to be a clear linear relationship, the experimental data do not extrapolate to the origin as would be predicted by theory. It may be that as the sample volumes become smaller the portion of the stored energy that is distributed into fractures is no longer constant. As data later in this article will show, this seems to be particularly true for the thinnest samples (1.6 mm thick).

We also attempted to fracture 9.6 mm thick plates however they proved exceedingly difficult to break. By use of multiple laser induced flaws as well as water vapor added to promote slow crack growth, we were eventually able to propagate one crack to catastrophic failure. The fracture area generated during the catastrophic portion of crack growth was about 15 cm^2. This datum is not shown in Fig. 3 since it is only a single point; however in a later section we compare this result with the fracture results from the other plates.

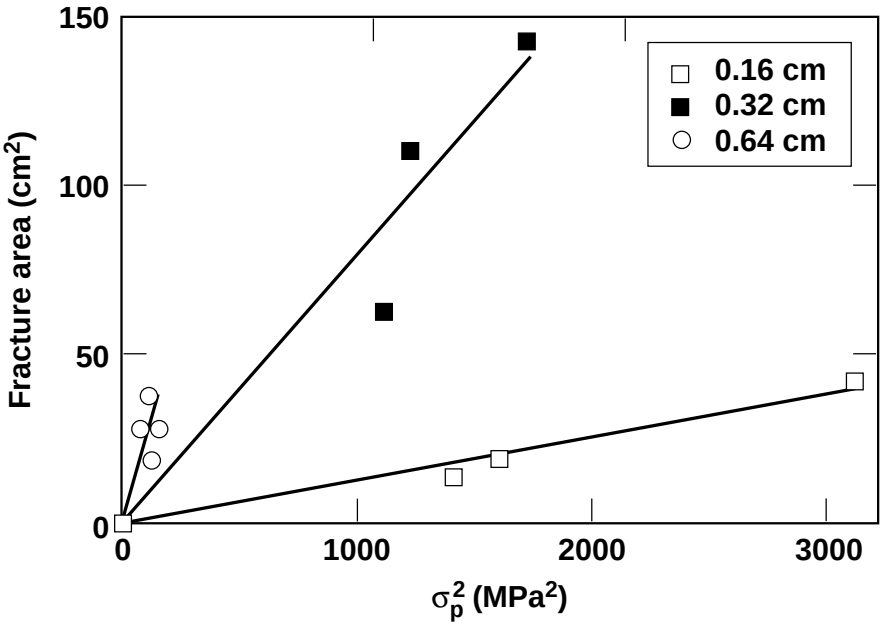

Figure 3. Measured fracture area versus the square of the peak stress (σ_p^2) for fused silica plates of different thickness. The lines through the points are from linear regression analyses of the data and constrained to pass through the origin.

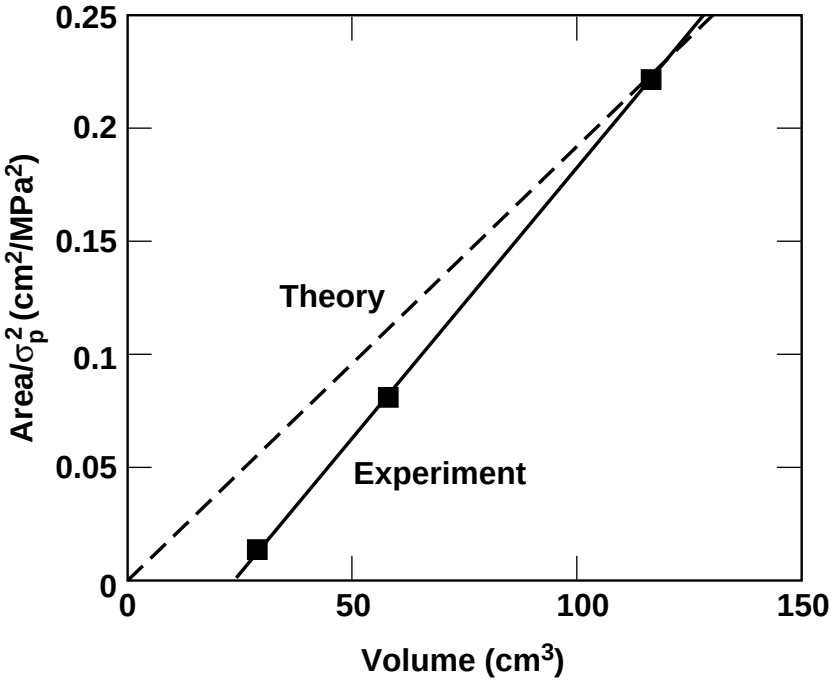

Figure 4. The change in fracture area per peak stress squared (i.e. the slope of the lines shown in Figure 3) versus the sample volume. The solid line is from a linear regression analysis; the dashed line is the assumed theoretical dependence discussed in the text (see eq. 6).

B. Measured fracture areas for Nova and Beamlet lenses

In earlier work[8] we measured the fracture area generated by a number of failed Nova lens and used equation 7 to describe the data. It is quite simple to measure the post-failure fracture areas of Nova lenses because they do not implode. Fig. 5 shows typical examples of failed Nova spatial filter lenses (σ_p = 810 psi [5.5 MPa]) that have fractured into either two or three pieces. The damage sites producing the failure are clearly seen in the figure and correspond closely to the critical flaw depth predicted for failure (i.e. about 6 mm deep); these lenses are 52 cm in diameter and 3.7 cm thick at the center.

On two occasions, damage to Beamlet spatial filter lenses has resulted in catastrophic failure leading to implosion. The lenses were 61 cm in diameter and 3.5 cm thick (peak stress =1490 psi[10.1MPa]). Unfortunately, no large lens fragments remained intact after the first implosion so it was impossible to recreate the fracture pattern (i.e. fracture area) at the time of failure. After the second implosion, however, a number of sizable glass fragments remained lodged in the mount (Fig. 6). Careful post failure analysis, using accepted fractology methods,[11,12] has allowed us to determine the probable fracture pattern of the lens (Fig. 7). This analysis shows that the lens failure probably produced between 9 to 11 large radial fractures, some of which were undoubtedly the result of crack branching from the initial fracture that grew from the damage site. This fracture pattern was determined by analyzing the Wallner lines and other fracture growth characteristics left on the fracture surfaces. In addition we compared the spacing between the primary radial fractures shown in Fig. 7 with the value predicted for a uniform distribution of radial cracks (Fig. 8). Note that the initial fractures project in a radial pattern from a point near the center of the lens. This suggests that the laser induced damage that initiated the failure also occurred at or near the center of the lens; this point has been confirmed by other data collected from the laser shot.

C. Comparison of fracture areas measurements

The above fracture analysis of the Beamlet lens allows us to compare the measured lens fracture area with that predicted based on eq. 7; the agreement is quite good (Fig. 9). We also compared the predictions with the measured fracture areas for the small 15-cm diameter test plates. This data is shown in Fig. 10 where the measured fracture area is plotted versus the predicted value from eq. 7 for the Nova and Beamlet lenses as well as for the 15-cm diameter test plates. The predicted and measured fracture areas are in good agreement over a wide range in sample volume (more than 10^2). The only exceptions are the fracture measurements made on the thinnest glass plates (15 cm dia. x 1.6 mm thick). In this case, eq. 7 over-predicts the degree of fracture. We expect that this is due to a change in the fraction of the stored energy that generates new surfaces (i.e. fractures). The data tend to support this reasoning; note that the points for the 1.6 mm thick samples run nearly parallel to main diagonal line but are offset by a constant value. Furthermore the data presented earlier (Fig. 4) show that the samples with the smallest volume produce less fracture than expected theoretically.

(a)

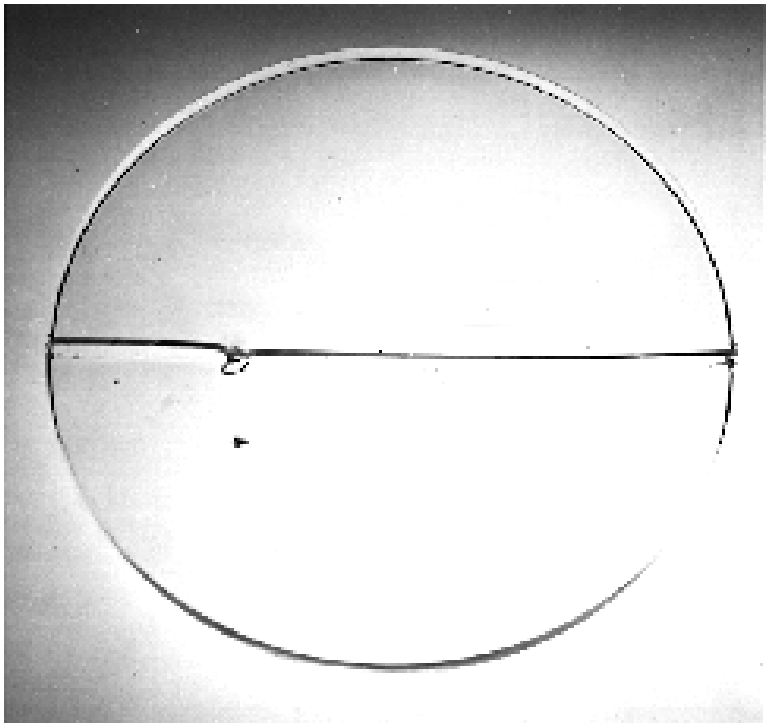

(b)

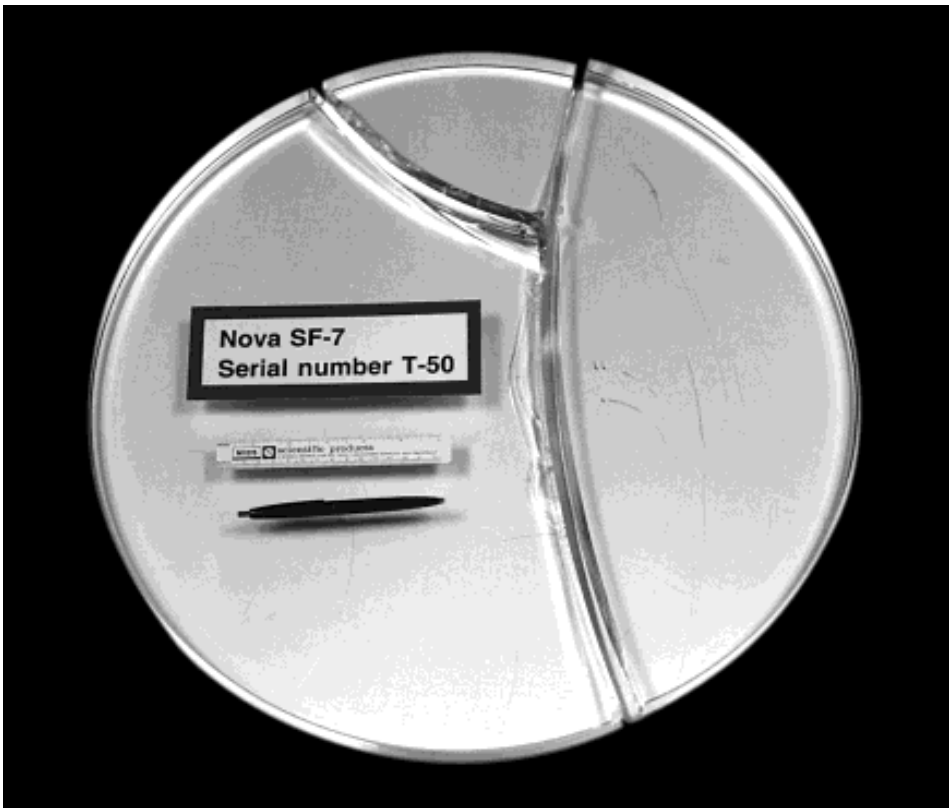

Figure 5. Photograph showing two 52-cm diameter Nova spatial filter lenses after catastrophic failure in which the lenses broke into either (a) two or (b) three pieces.These lenses did not implode but bridged" the opening of the spatial filter vacuum vessel. The peak stress in these lenses was 810 psi (5.5 MPa).

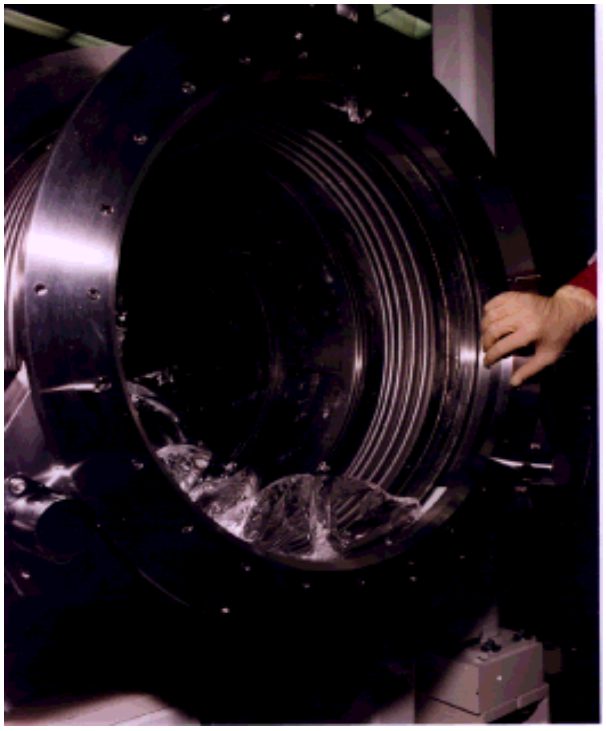

Figure 6. Photograph showing some of the remaining fragments following the implosion of a 61 cm diameter Beamlet vacuum spatial filter lens.

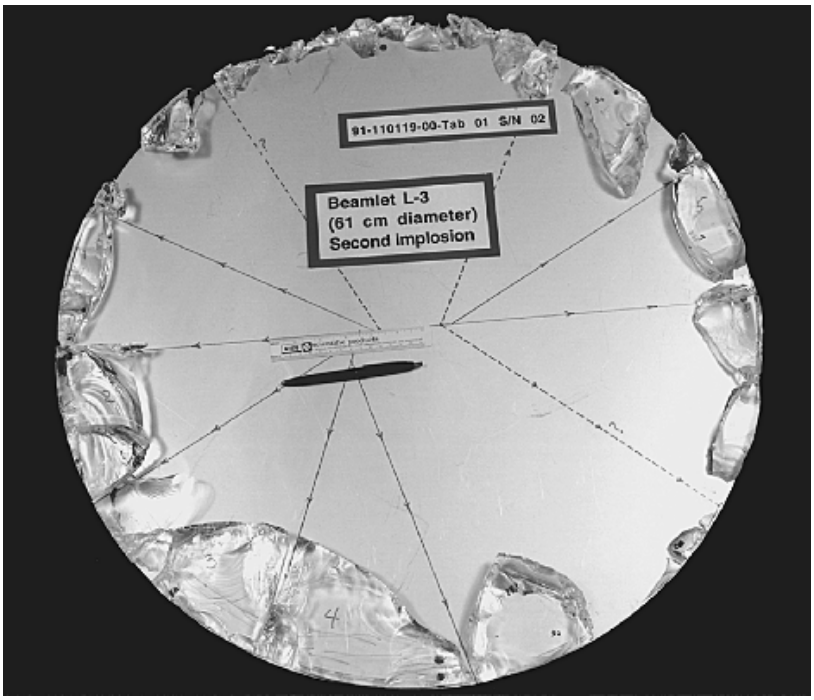

Figure 7. The fragments shown in Fig. 6 plus other fragments that comprised the border of the lens, were reassembled and used to determine the initial fracture pattern of the lens. Note that the fractures appear to have originated at a critical flaw site near the lens center; this agrees with other non-fracture data collected after the incident. The peak tensile stress in the lens was 1490 psi (10.1 MPa).

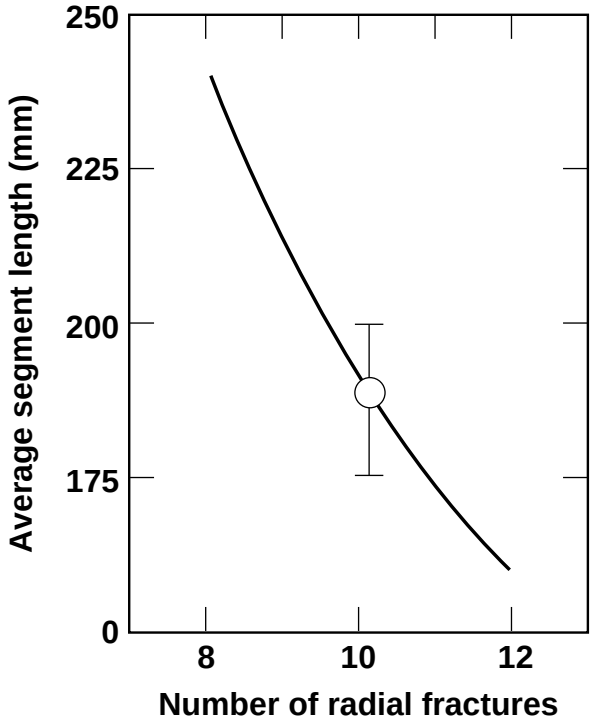

Figure 8. Plot of the mean spacing between radial fractures versus the number of fractures produced for the 61-cm diameter Beamlet lens (circumference 162 cm). The average fracture spacing, based on the reassembled fragments (Figure 7), is 187 $\pm$ 15 cm suggesting that 9 -11 large radial fractures were generated at the time of failure.

The good agreement between the predicted and measured degree of fracture over such a wide range in window sizes suggests that eq. 7 can be used with reasonable confidence to design vacuum barrier optics that will not implode. This, of course, is with the caveat that the optics being designed are similar in shape and material to those used in this study.

D. Design criteria for a “fail-safe” vacuum barrier optic

Based on the results given above, it is possible to specify a peak design stress for a “fail-safe” vacuum barrier optic. We use the term “fail safe” to mean the optic will not implode but instead will break into a maximum of only two fragments. Based on eq. 7 and the data shown in Fig. 9, we have chosen a safe peak design stress of 500 psi (3.5 MPa) for the lenses and windows that are used as vacuum barriers on the large LLNL Fusion lasers. At this stress, the stored energy is insufficient to propagate more than one full-diameter crack (i.e. 2 radial fractures) thus preventing an implosion. This stress also allows about a factor of two safety margin. This safety margin accounts for the uncertainty in the measurements from which eq. 7 was developed and also allows some latitude for refinishing the lens to remove minor damage or imperfections that may appear during operation. The ability to refinish lenses represents a significant operational cost savings, however, one must be careful to plan for the effect of the decrease in the lens thickness (after refinishing) on the peak tensile stress.

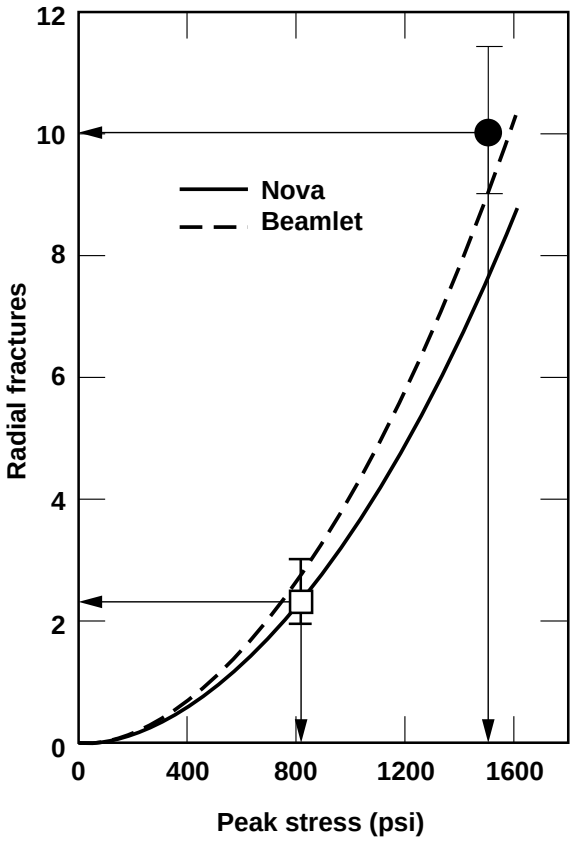

Figure 9. Fracture area versus peak tensile stress for Nova and Beamlet spatial filter lenses (based on eq. 7). The two points represent the average as well as the range of data for eight failed Nova lenses plus the single data for the imploded Beamlet lens shown in Fig. 6 and 7. The error bars on the Beamlet datum represent our estimate of the error in determining the number of radial fractures produced at the time of failure.

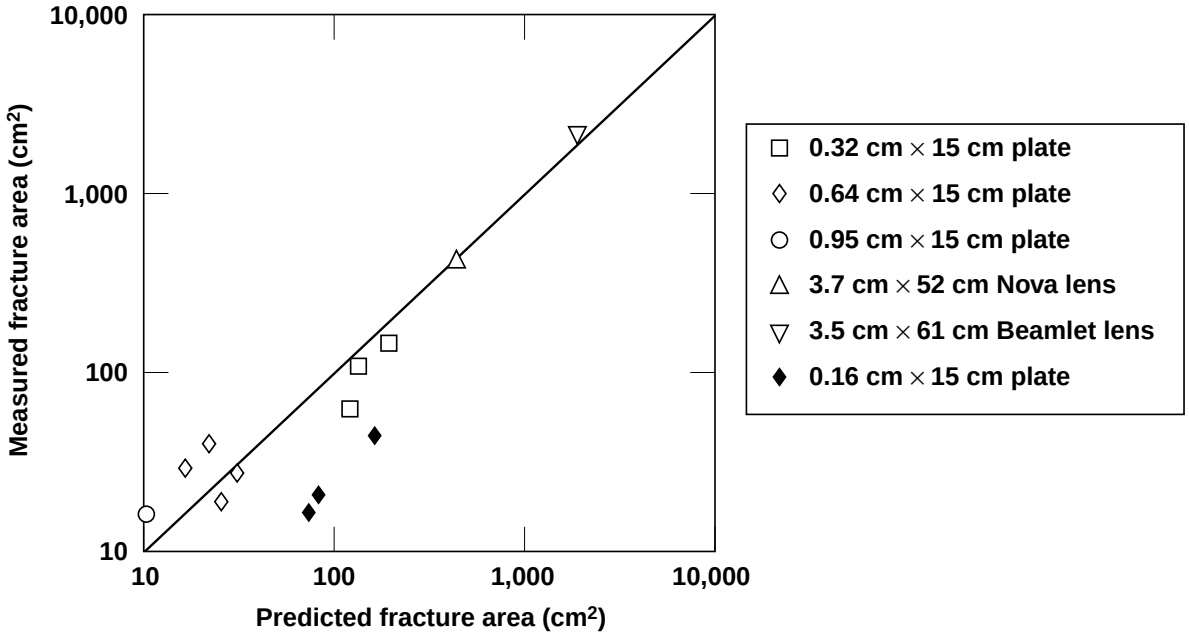

Figure 10. Comparison of the measured fracture area versus that predicted by eq. 7; the data are for a series of glass plates of varying diameter and thickness as well as Nova and Beamlet lenses.

To develop a safe lens design one must also consider the ratio of the critical-flaw-size to window thickness. This is particularly true for small windows where the 500 psi limit may be too conservative. For example, at a tensile stress of 500 psi the critical flaw size is about 15 mm for fused silica. If the optic is <15 mm thick then a critical flaw size of 15 mm loses physical meaning. Based on our experience (Table 1), we suggest that the ratio of lens thickness (t) to critical flaw size(r_c) be less than 6.

Table 1. Comparison of the ratio of thickness to critical flaw size (t/r_c) for various vacuum optics in this study.

Lens/window	Peak stress (psi)	Peak stress (MPa)	Thickness t (mm)	Flaw size r_c (mm)	t/r_c	No. of radial fractures
Beamlet L3	1490	10.1	35	2.1	16.7	9-11
Nova SF-7	810	5.51	37	5.5	6.7	2-3
Nova 3ω focus	515	3.50	83	15	5.5	<1
15-cm SiO_2 plate	830	5.65	9.5	5.4	1.8	≤1

We currently have in operation large vacuum barrier optics that meet the above two design criteria: i.e. peak tensile stress of 500 psi and $t/r_c < 6$. These are the 80-cm diameter Nova final focus lenses; these lenses have a peak tensile stress of about 510 psi (3.5 MPa). Over more than 10 years of high fluence operation on Nova, these lenses have, at times, experienced extensive damage. In particular, in the early years of operation we found that stimulated Brillouin scattering indirectly caused large damage spots at the center of these lenses. In the worst cases this damage consisted of elliptical shaped cracks on the tensile surface of the lens that, in some instances, exceeded 3-cm in length. At no time did we observe catastrophic crack growth in these lenses. In fact the lens with the worst damage was off-line pressure tested up to a load of 23 psi (0.15 MPa) and found to fail only after repeated pressure-and-hold cycles; the calculated peak stress at failure was 805 psi (5.5 MPa).

E. The role of secondary crack growth

During the course of this work we also carried out fracture experiments on 15 cm diam. x 0.64 cm thick samples of borosilicate glass. The particular borosilicate glass used had a fracture toughness nearly equivalent to that of fused silica (~0.75MPa•$m^{1/2}$).

The purpose of these experiments was to improve the statistics of measured fracture area at peak stresses near 2000-2500 psi (13.5 to 17.0 MPa). However, we observed a 4-fold variation in the measured fracture area (Fig. 11) even though the stress at failure varied only from about 2100 to 2400 psi (14.2 to 16.3 MPa)! During these tests we also observed that the noise produced at the time of failure was louder when more fractures were generated; subsequent measurements of the peak audio signal during fracture showed that the fracture area and the audio output energy were linearly correlated (Fig. 12). At first these observations appear to violate the energy conservation

law given by eq. 8. This is because the quantity of stored energy remains nearly fixed (stress is approximately constant) yet the amount of energy released as audio energy and as new surfaces (i.e. fractures) both increase. In addition we observed that the fractures produced either 2, 3 or 4 main fragments that we classified as Type I, II, or III, fracture patterns, respectively (Fig. 13). All three patterns appear to be related; note that the main fractures all originate at the flaw site and then propagate radically to the edge of the plate.

To explain this phenomena we propose that, in this relatively low stress region, catastrophic fracture occurs in a sequence of discrete steps with each step producing at least one radial fracture. Between fracture steps the stress (and stored energy) changes in the segments. If the new stress distribution exceeds the critical stress at the original flaw site then a new radial fracture is generated. This multi-step mechanism is schematically shown in Fig 14. This mechanism explains why the audio output energy should increase with the fracture area: each fracture step can be considered as a separate event drawing from the new stored energy distribution.

A key question is whether the stress increases at what remains of the original flaw site after the first full diameter fracture is generated. This point is illustrated more clearly by step II of the mechanism as shown in Fig. 14. After the first full fracture has propagated, the criteria for further crack growth is that either σ_{p2}' or σ_{p2}'' or both exceed the critical strength at the flaw site. We examined whether this is possible by modeling the stress distribution in the two halves of a fractured test plate using the finite element stress-strain code NIKE-3D. The sizes of the two glass segments used in the calculations were based on pieces recovered after a type I failure of a 15-cm test part. Fig. 15 shows the calculated peak stresses at the flaw for both fracture segments. Prior to fracture the peak stress in the plate is 2300 psi (15MPa) whereas after fracture the stresses at the flaw in each of the two halves increase nearly 50% to about 3800 psi (25.9MPa). If the flaw that remains in each segment exceeds the critical flaw size for this new stress distribution then a second fracture will propagate. We refer to the subsequent fracture steps as “secondary” crack growth. This secondary crack growth explains why we observe the family of fractures shown in Fig. 13 and also the fracture pattern observed in Nova lenses (see Fig. 5).

An important consequence of the proposed fracture mechanism is that the extent of secondary fracture depends strongly on how long the load is maintained on the remaining fragments. After the first fracture is generated, the two pieces it produces will have a tendency to lock in place and the vacuum load may or may not be rapidly removed depending on the leak rate and size of the system. This may be a critical issue in the design of windows for very large vacuum systems. In such cases the fragments may lock-up and remain under load for several hours. Under these conditions the chance for further fracture increases due to slow, sub-critical crack growth that is enhanced by both the prolonged vacuum load and the intrusion of water vapor into the vacuum. Thus secondary crack growth could eventually lead to an implosion if the load remains on the bridging segments for a prolonged period of time.

The consequence of secondary crack growth on the failure of windows in other applications (e.g. aircraft, space craft, etc.) has not escaped our attention. Note however that this sequential mechanism of fracture occurs only in plates loaded at relatively low stresses. That is, conditions under

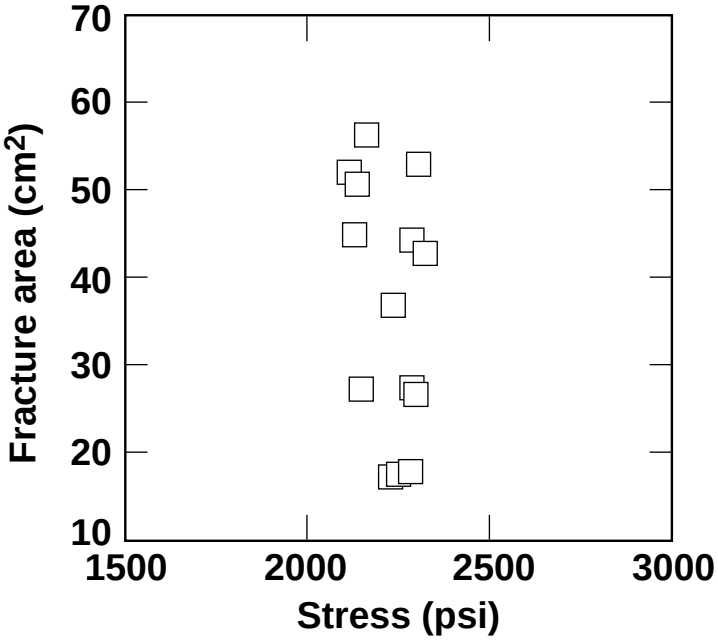

Figure 11. Measured fracture area vs. peak stress observed during tests on 15-cm diameter x 0.32-cm thick plates of a Pilkington borosilicate glass.

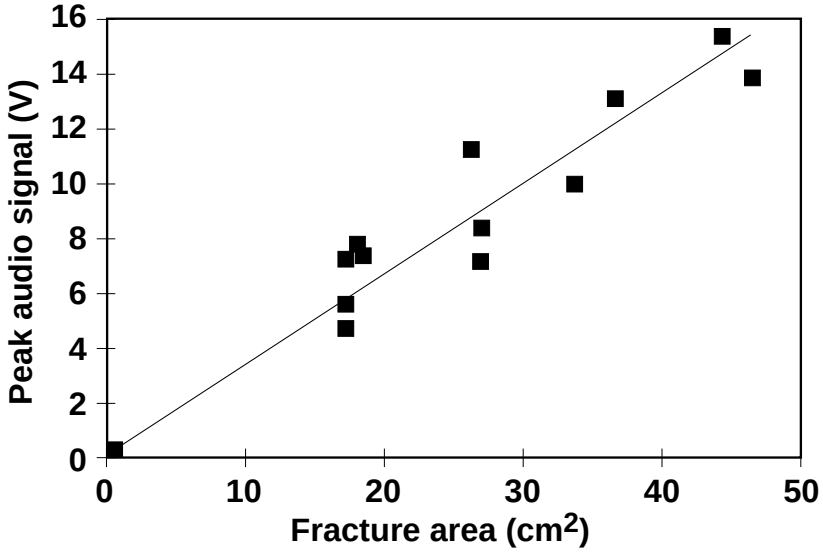

Figure 12. Audio signal output at the time of fracture vs. measured fracture area.

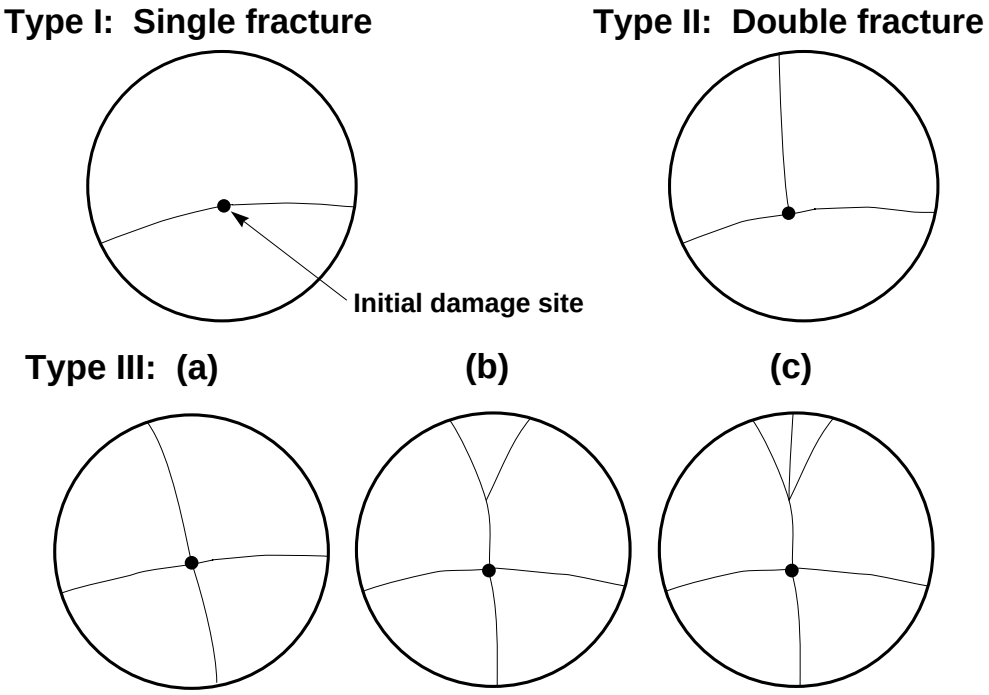

Figure 13. Three distinct fracture patterns observed during the tests on 15-cm x 0.32-cm thick plates of a borosilicate glass. The patterns are classified as type I, II or III depending on whether 2, 3 or 4 radial fractures originate at the flaw site.

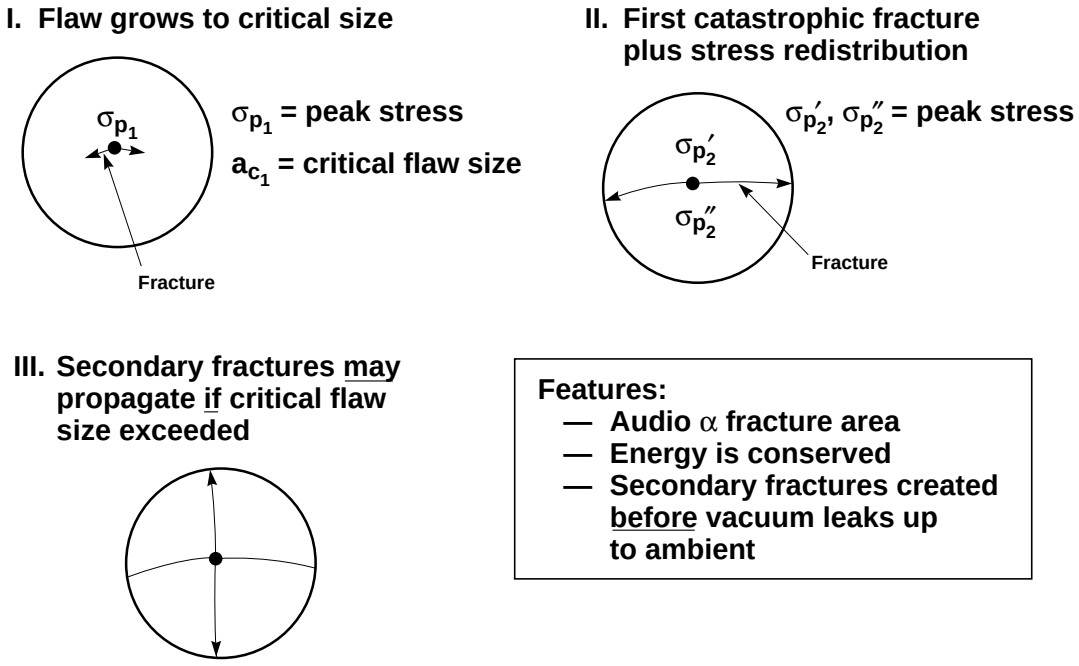

Figure 14. Proposed multi-step mechanism for the fracture of circular glass plates under relatively low stress conditions.

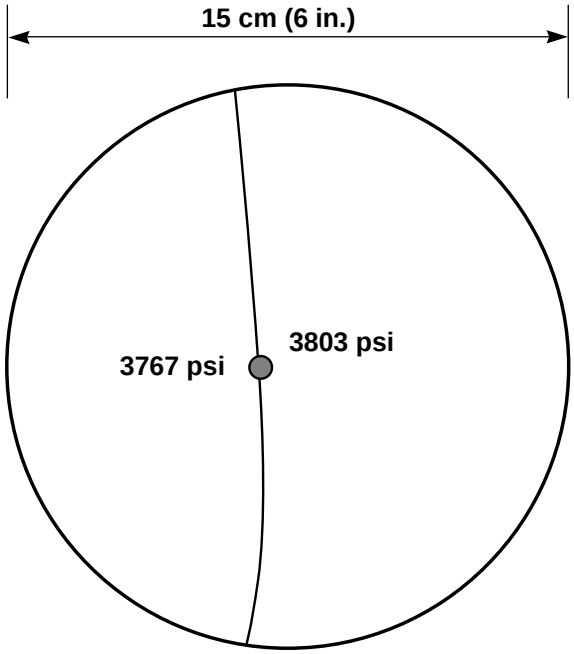

Figure 15. Peak stress calculated near the remnants of the original flaw in each of the two segments produced during fracture. There segments remain under vacuum load immediately after fracture.Prior to fracture the stress at the flaw site is about 2300 psi (15.6 MPa).

which failure produces only one or two large fractures allowing the remaining segments to lock in place. In contrast, at very high stress (high stored energy) the initial crack produced at failure rapidly branches into more cracks, producing too many pieces to support the vacuum load. In such cases an implosion ensues. The Beamlet lens is an example of this type of failure.

5. CONCLUSIONS

The design of a “fail-safe” lens for high peak power applications depends on three key factors. First, for large lenses the peak stress should be less than 500 psi. At this stress level only one full diameter fracture is produced and the two fragments lock in place. Although the vacuum is breached, no catastrophic implosion occurs. In addition the ratio of the lens thickness to critical flaw size should be less than six. Finally, it is desirable that the vacuum load be removed as rapidly as possible to avoid the possibility of secondary crack growth.

6. ACKNOWLEDGMENTS

This work is supported under DOE Contract number W-7405-ENG-48 with the University of California’s Lawrence Livermore National Laboratory. The authors gratefully acknowledge the helpful discussions with Dr. Suresh Gulati at Corning Inc.

7. REFERENCES

1. B. M. Van Wonterghem, J. R. Murray, J. H. Campbell, D. R. Speck, C. E. Barker, I. C. Smith, D. F. Browning and W. C. Behrendt, "Performance of a prototype, large-aperture multipass Nd-glass laser for Inertial Confinement Fusion," accepted for publication, *Applied Optics*.

2. National Ignition Facility Conceptual Design Report, Vol. 2 and 3, Lawrence Livermore National Laboratory, Report No. UCRL-PROP-117093, May 1994.

3. J. T. Hunt and D. R. Speck, "Present and future performance of the Nova laser system," *Opt. Eng.,* Vol. 28, pp. 461-468, April 1989.

4. W. W. Simmons, J. T. Hunt, and W. E. Warren, "Light propagation through large laser systems, *IEEE J. Quantum Electron,* Vol. QE-17, pp. 1727-1744, September 1981.

5. J. T. Hunt, J. A. Glaze, W. W. Simmons, and P. Renard, "Suppression of self-focusing through low-pass spatial filtering and relay imaging," *Appl. Opt.,* Vol. 17, pp. 2053-2057, 1978.

6. J. B. Trenholme, *1975 Laser Program Annual Report*, UCRL-50021-75, pp. 237-241, 1975.

7. J. B. Trenholme and J. T. Hunt, private communication, Lawrence Livermore National Laboratory, 1992.

8. J. H. Campbell, G. Edwards and J. Marion, "Damage and fracture in large aperture, fused silica, vacuum spatial filter lenses," *Solid-State Lasers for Application to Inertial Confinement Fusion*, SPIE Vol 2633, p. 522, June 1995.

9. J. Mencik, *Strength and Fracture of Glass and Ceramics,* Elsevier, New York, (1992), pp. 99-151.

10. S. W. Freiman, "Fracture mechanics of glass," Chap. 2, *Glass: Science and Technology,* Vol. 5, D. R. Uhlmann and N. D. Kreidl (eds), Academic Press, (1980), New York.

11. T. A. Michalske, "Quantitative fracture surface analysis," in *Engineered Materials Handbook*, Volume 4, Ceramics and Glasses, pp. 652-662, ASM International, Materials Information Society, (1991).

12. J. R. Varner, "Descriptive fractography," in *Engineered Materials Handbook,* Volume 4, Ceramics and Glasses, pp. 635-644, ASM International, Materials Information Society, (1991).

13. M. Feit, A. M. Rubenchik, D. R. Faux, R. A. Riddle, D. C. Eder, B. M. Penetrante, D. Milam, F. Y. Genin and M. R. Kozlowski, “Modeling of laser damage initiated by surface contamination”, *Laser Induced Damage in Optical Materials: 1996*, SPIE, Boulder, CO, October 7-9, 1996 (in this proceedings).

14. S. M. Weiderhorn, J. *Am. Ceram. Soc.*, 50, (1967), pp. 407-414.